Electron Temperature Fluctuations and Turbulent Heat Fluxes in the DIII-D SOL

D.L. Rudakov[1], J.A. Boedo[1], R.A. Moyer[1], P.C. Stangeby[2], G.R. Tynan[1], and J.G. Watkins[3]

[1]*University of California San Diego, La Jolla, California 92093-0417, USA.*
[2]*University of Toronto Institute for Aerospace Studies, Toronto, M3H 5T6, Canada.*
[3]*Sandia National Laboratories, Albuquerque, New Mexico 87185, USA.*

1. Introduction

The scrape-off layer (SOL) width in a tokamak is generally determined by the balance of perpendicular (across toroidal magnetic field, B_T) and parallel transport of particles and energy [1]. Of particular importance to future fusion devices like ITER and DEMO is the so-called SOL power width, i.e. parallel power flux density e-folding length, λ_q, which is one of the major parameters determining the peak power load on the divertor and limiter surfaces. The cross-field transport of particles and heat in the tokamak edge and SOL is largely due to the fluctuating $E \times B$ velocity due to electrostatic turbulence (e.g. [1,2] and references therein). Correlated fluctuations of the plasma radial velocity v_r, density n, and temperature T_e result in time-average fluxes of particles and heat given by (for electrons) [3]:

$$\Gamma_r^{ES} = \langle n\tilde{v}_r \rangle = \frac{1}{B_\varphi}\langle \tilde{n}\tilde{E}_\theta \rangle; \quad Q_r^{ES} = \langle nT_e\tilde{v}_r \rangle \approx \frac{3}{2}kT_e\Gamma_r^{ES} + \frac{3}{2}\frac{n_e}{B_\varphi}\langle k\tilde{T}_e\tilde{E}_\theta \rangle = Q_{conv} + Q_{cond},$$

where Q_{conv} and Q_{cond} are, respectively, convective and conductive heat fluxes. Experimental determination of these fluxes requires simultaneous measurements of the density, temperature and poloidal electric field fluctuations with high spatial and temporal resolution. Langmuir probes provide the most readily available (if not the only) tool for such measurements. However, fast measurements of electron temperature using probes are non-trivial and are not performed routinely in most tokamaks. Thus the contribution of T_e fluctuations to turbulent fluxes is often neglected. In DIII-D a fast T_e diagnostic has been deployed and routinely operated since 1999. Below we present an overview of T_e fluctuation and turbulent heat flux measurements under varying discharge conditions.

2. Experimental arrangement

Figure 1(a) shows poloidal cross-section of DIII-D with last closed flux surfaces of lower single null (LSN) and inner wall limited (IWL) magnetic configurations. T_e fluctuations and fluctuation-induced transport are studied in edge and SOL plasmas of the DIII-D tokomak [4] using a reciprocating Langmuir probe array (RCP) [5] equipped with a fast (100 kHz bandwidth) T_e diagnostic [6]. The diagnostic is based on detection of harmonics

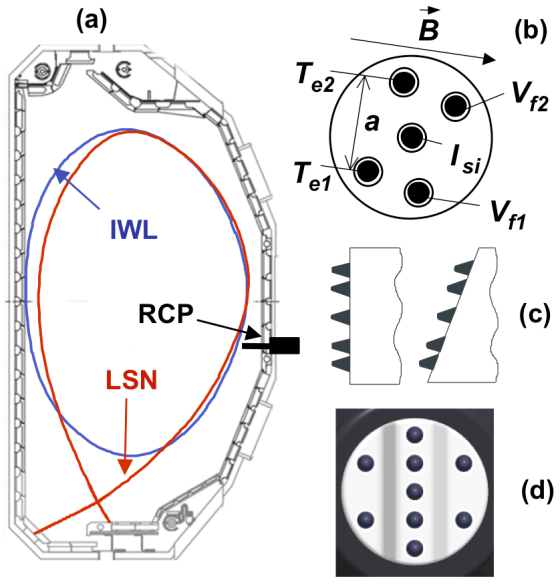

Fig. 1. Experimental arrangement in DIII-D.

in the current spectrum of a fast-swept single probe [7]. The novel features of the diagnostic at DIII-D include active voltage feedback and fully digital data processing [6]. The probe head layout used prior to 2011 is shown in Fig. 1(b). It consisted of 5 tips including an ion saturation current (I_{si}) tip, two floating potential (V_f) tips, and two T_e tips separated by $a \approx 9.3$ mm in the poloidal direction. The head was oriented to achieve the best possible alignment of V_f and T_e tips without mutual shadowing. The probe enters the DIII-D SOL 18.8 cm below the outer midplane, where poloidal cross-section of the last closed flux surface is typically inclined with respect to vertical by 11%–17% [Fig 1(a)]. Prior to 2003 the probe face was cut vertical in the poloidal plane [Fig. 1(c), left]; in 2003 it was modified to better conform to the flux surfaces [Fig. 1(c), right]. Furthermore, in 2011 the probe shaft and head were upgraded to 9 tips [Fig. 1(d)].

3. Electron temperature fluctuations in the DIII-D SOL

Edge T_e fluctuations in DIII-D have been studied in and low (L-) and high (H-) confinement mode discharges. The fluctuations have normalized levels ranging from 0.1–0.2 at the separatrix to 0.5–0.6 in the SOL [8,9], comparable to the respective levels of the density and floating potential fluctuations. The fluctuations are broadband with significant energy throughout the measurable range (up to 100 kHz) [9]. T_e fluctuations tend to be roughly in phase with the electron density (n_e) fluctuations and about 90° out of phase with V_f fluctuations [9].

Both absolute and relative T_e fluctuation levels tend to increase with the discharge density. This is illustrated in Fig. 2 showing radial profiles (vs the distance from LCFS) of the temperature fluctuation levels in a low density (n_e/n_{GW}=0.25, where n_{GW} is Greenwald density) L-mode discharge (magenta), high density (n_e/n_{GW}=0.6) L-mode discharge (green) and a high-density (n_e/n_{GW}~1) H-mode discharge (red). All discharges were LSN with toroidal magnetic field B_T = 2.1 T, plasma current I_p = 1.1 MA and power into SOL (equal to input power minus power radiated from the plasma core) $P_{SOL} \approx$ 1.1 MW. T_e fluctuation levels are clearly higher in the higher density L-mode case compared to the lower density

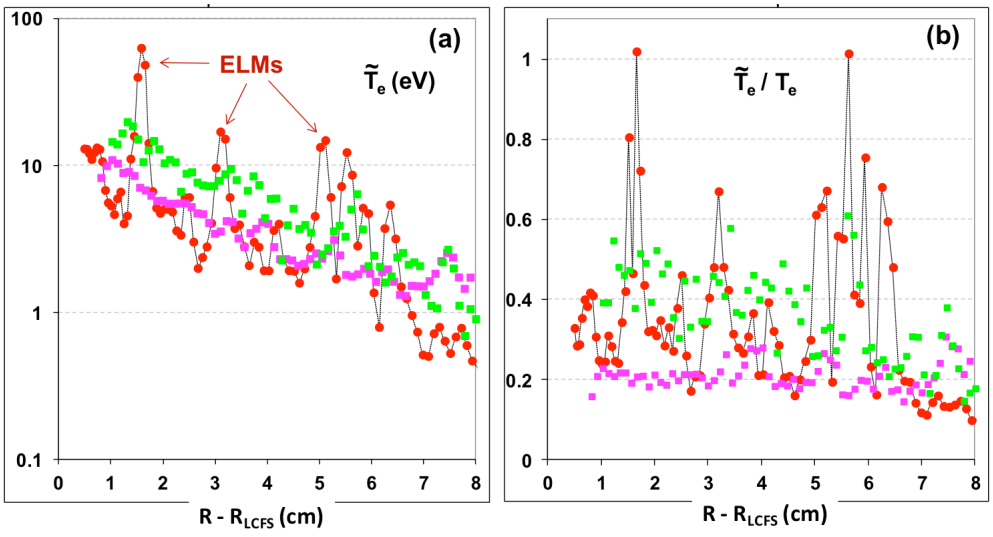

Fig. 2. Radial profiles of the absolute (a) and relative (b) T_e fluctuation levels in L- (magenta, green) and H- (red) modes.

one. In H-mode between edge localized modes (ELMs) absolute T_e fluctuation levels are lower than in both L-mode cases, while during ELMs they increase to above L-mode levels, with relative levels reaching $\tilde{T}_e^{rms} / T_e = 1$. Immediately after L-H transition, T_e fluctuation levels are typically quenched, as illustrated in Fig. 3. Shown are probe position (a), mean T_e (b) and absolute (c) and relative (d) fluctuation levels. While there is little change in the mean T_e immediately after the transition (at least at the probe location), the fluctuation levels decrease by more than a factor of 2, with the relative level dropping from 0.4–0.5 to ~0.2.

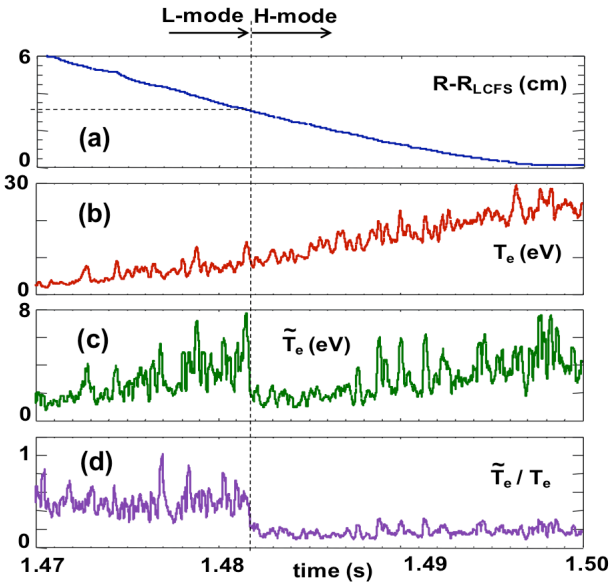

Fig. 3. Temporal evolution of T_e fluctuation levels across L-H transition.

4. Fluctuation-driven heat fluxes and power balance in DIII-D SOL

Both convective and conductive components of the fluctuation-driven heat flux are routinely measured in L- and H-mode discharges. Figure 4 shows representative profiles of the convective (circles) and conductive (diamonds) cross-field heat fluxes in IWL (a) and LSN (b) L-mode discharges. The two components tend to be comparable near the LCFS, while in the far SOL of IWL discharge the convective component tends to be larger. This may be a consequence of significant part of the heat flux being carried by intermittent convection of plasma blobs [8,9]. In the near SOL, blobs produce correlated spikes in n_e, T_e, and radial velocity ($v_r = E_\theta \times B$) measured by the probe. As the blobs propagate through the SOL, they lose energy faster than density, thus correlation between T_e and v_r spikes is lost faster than that between n_e and v_r spikes. Consequently, the conductive component of the heat flux is reduced stronger than the convective one. Note that the SOL power width is substantially higher in IWL compared to LSN [10].

If fluctuation-driven cross-field transport is indeed the dominant mechanism of the energy loss across the LCFS, the integral of the radial heat flux measured at LSFS, Q_{rLCFS}, over the LSFS area should be approximately equal to P_{SOL}. Figure 5 shows a dependence of the measured Q_{rLCFS} in IWL (blue triangles) and LSN (red circles) L-mode discharges on P_{SOL}. Assuming poloidally uniform heat transport and taking LCFS area

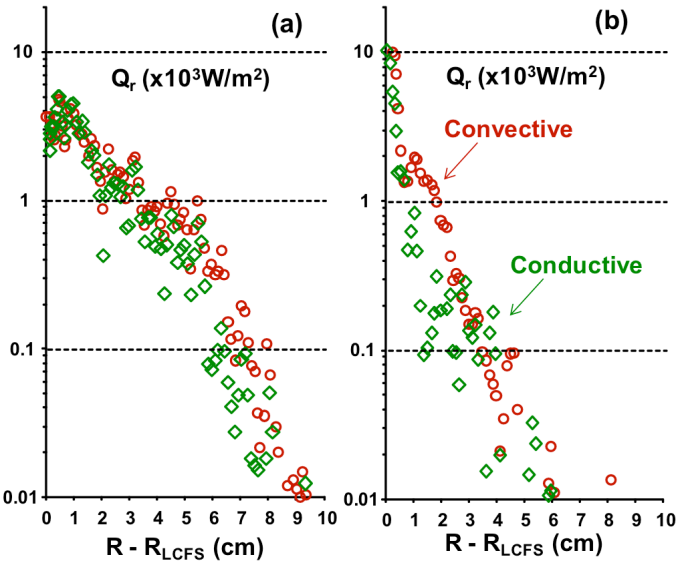

Fig. 4. Radial profiles of the convective and conductive cross-field heat fluxes in IWL (a) LSN (b) L-mode.

to be $S_{LCFS} \approx 40$ m^2, one gets the expected dependence shown by the dashed line in Fig. 5. The line is in good agreement with the measured data, with scatter less than a factor of 2, which is within the error bars of the heat flux measurement. This result contrasts with the previously reported measurements [9], where measured cross-field fluxes were significantly higher, and a toroidal band near the outer midplane having poloidal width of about 1 meter would be sufficient to conduct power equal to P_{SOL}. Those earlier results were obtained with a probe head not well conforming to magnetic flux surfaces [as in Fig 1(c), left]. Apparently, radial separation of the tips led to overestimation of the fluxes. With the new head design the results appear more physical. On the other hand, it is widely believed that the radial transport is stronger on the low-field side (consistent with BOUT modeling [11]), so one would expect measured cross-field transport on the outboard mid-plane to be somewhat higher than P_{SOL}/ S_{LCFS}. Measurements at multiple poloidal locations would be needed to address this issue. X-point reciprocating probe located in the lower divertor and newly installed swing probes on the center post may be used in the future for comparison with midplane data reported here.

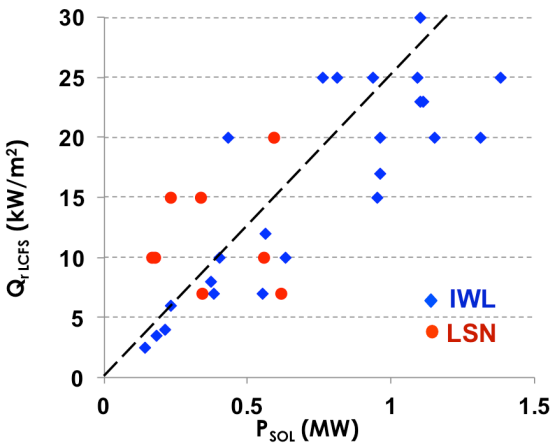

Fig. 5. SOL power balance in IWL and LSN L-mode.

5. Summary

Electron temperature fluctuations are routinely measured in the SOL of DIII-D using reciprocating Langmuir probe array. T_e fluctuations have levels comparable to those of the density and floating potential fluctuations. Fluctuation-driven cross-field heat transport consists of the convective and conductive components that are comparable near LCFS in L-mode. Overall measured cross-field heat transport is roughly consistent with power balance in L-mode. Poloidal asymmetries of the cross-field heat transport will be assessed in the future work.

This work was supported in part by the US Department of Energy under DE-FG02-07ER54917, DE-FC02-04ER54698, and DE-AC04-94AL85000.

References

[1] P.C. Stangeby and G.M. McCracken, Nucl. Fusion **30**, 1225 (1990).
[2] M. Endler, J. Nucl. Mater. **266–269**, 84 (1999).
[3] D.W. Ross, Plasma Phys. Control. Fusion **34**, 137 (1992).
[4] J.L. Luxon, Nucl. Fusion **42**, 614 (2002).
[5] J.G. Watkins et al., Rev. Sci. Instrum. **63**, 4728 (1992).
[6] D.L. Rudakov, J.A. Boedo, R.A. Moyer, et al., Rev. Sci. Instrum. **72**, 453 (2001).
[7] J.A. Boedo, D. Gray, R.W. Conn, et al., Rev. Sci. Instrum. **70**, 2997 (1999).
[8] D.L. Rudakov, J.A. Boedo, R.A. Moyer, et al., Plasma Phys. Control. Fusion **44**, 717 (2002).
[9] D.L. Rudakov, J.A. Boedo, R.A. Moyer, et al., Proc. 30th EPS Conference on Controlled Fusion and Plasma Physics, St Petersburg, Russia 2003 ECA Vol. 27A, P-4.87.
[10] D.L. Rudakov, J.A. Boedo, R.A. Pitts, et al., J. Nucl. Mater. **415**, S387 (2011).
[11] X.Q. Xu et al., Nucl. Fusion **40**, 731 (2000); New J. Phys. **4**, 53.1 (2002).